Chapter 4

Self-assembling Conjugate of LSF- Linoleic Acid (LA)

1. Introduction

As discussed previously in **chapter 2**, LSF has significant clinical potential but it poses certain major challenges that limit its clinical development, including high aqueous solubility (~60 mg/mL in water) which hinders its encapsulation in any delivery system.[1] LSF is reported to be orally non-bioavailable and is hence administered at a high dose of 25 mg/kg twice daily in T1DM animals [1,2] and in clinical trials, at single dose of 12 mg/kg by a continuous subcutaneous (s.c.) or i.v. infusion over 24 hours due to its rapid metabolism and an extremely short half- life. [3-5] LSF also undergoes rapid metabolism to form metabolite PTX and this LSF-PTX interconversion is mainly responsible for the high dose of LSF.[6]

Inspite of being a potent molecule, it is quite less explored and very few reports are available in literature focusing on the physicochemical and PK issues associated with LSF. In one such study, Cui et al. have synthesized 32 analogs based on the structural motif of LSF wherein, only two of these analogs were found to be effective in protecting β-cells from cytokine-induced injury and maintaining insulin secretory ability in cell culture based evaluation. Nonetheless, no *in vivo* PK and pharmacodynamics data is reported on these analogs to determine if the synthesized analogs improved the metabolic stability and oral bioavailability of LSF.[7] We did not come across any other study focusing upon the approaches to modify LSF or to deliver it by either conventional or novel drug delivery systems to overcome these challenges associated with the molecule.

Our objective was to overcome the physicochemical and PK limitations associated with LSF. For this purpose, we designed a LSF-fatty acid conjugate which could self-assemble into micelles in nano size range. This would enable hydrophobization of the drug, increase in its mean residence time in the body, and reduce LSF-PTX interconversion. LSF-PTX interconversion is only possible because LSF has a secondary hydroxyl group in its side chain that can oxidize into

ketone group and form metabolite PTX. In this work, we protected the hydroxyl group by conjugating LSF with a fatty acid that is linoleic acid (LA) via ester bond formation. This approach offers possible advantage that the resulting molecule (LSF-LA conjugate) would be amphiphilic in nature as LSF is hydrophilic and LA is hydrophobic. Being amphiphilic in nature, it might self-assemble into micelles which would further improve the PK and therapeutic efficacy of LSF.

For conjugating LSF, an essential fatty acid (EFA), linoleic acid (LA) was selected as a hydrophobic moiety. EFAs are fatty acids that humans and other animals require for good health however, cannot synthesize them and hence these need to be supplemented from external sources. Two such fatty acids, known for human beings, include alpha-linolenic acid (ALA) (18:3, omega-3 (ω-3)) and linoleic acid (LA) (18:2, omega-6 (ω-6)).[8] Linoleic acid was chosen for conjugation with LSF as it has similar molecular weight (280.3 g/mol) as LSF.[9] Additionally, it possesses anti-inflammatory activity *in vivo.*

In present work, we synthesized LSF-LA conjugate and characterized it by various spectroscopic and analytical techniques. LSF-LA conjugate was assessed for its self-assembling ability and particle size, size distribution, critical micellar concentration (CMC), micelle aggregation number (N_{agg}) and protein-micelles interaction (using BSA as protein) and for its efficacy in *in vitro* cell culture studies. For *in-vitro* efficacy testing, LSF-LA conjugate was incubated with insulin secreting murine cells, MIN-6 and evaluated for cytotoxicity. Further MIN-6 cells were exposed to inflammatory challenge with cytokines and protective effect of LSF-LA conjugate on cell viability and insulin secretion was studied. It was also tested for its ability to suppress PBMC proliferation and inflammatory cytokine production as well as cellular uptake. Further, PK of LSF-LA conjugate and free LSF was performed to determine the improvement in PK parameters and *in-vivo* efficacy was evaluated in STZ induced T1DM wistar rat model. To our

knowledge, this is the first report on self-assembling nano-drug delivery system for LSF using the drug-fatty acid conjugation strategy. Self-assembly of LSF-LA conjugate into micelles also reduced the dose since micellar formulations are known to prolong the circulation time and significantly decrease the metabolism and renal clearance of the encapsulated drugs.[10]

2. Materials and methods

2.1. Materials and reagents

LSF (purity >98%) was synthesized *in house* as per *chapter 2*. HPLC grade solvents, acetonitrile, methanol and DCM were obtained from Merck (Mumbai, India). Dulbecco's Modified Eagle Medium (DMEM), Fetal Bovine Serum (FBS), TrypLE and recombinant proteins (TNF-α, IL-1β and IFN-γ) were obtained from Invitrogen (USA); LA (purity ≥99%), Streptozotocin (STZ), 3-Isobutyl-1-methylxanthine (IBMX; ≥99%; Internal standard), 3-[4,5-dimethylthiazol-2-yl]-2,5-diphenyltetrazolium bromide (MTT) Cetylpyridinium chloride and D-glucose were purchased from Sigma Aldrich (USA). ELISA kits for TNF-α and IFN-γ (ELISA MAX^{TM}) were obtained from BioLegend (USA). Carboxyfluorescein succinimidyl ester (CFSE) staining assay kit (CellTrace™), Ficoll-Paque GE Healthcare and Phytohaemagglutinin (PHA) were obtained from ThermoFisher (USA). N-(3-Dimethylaminopropyl)-N′-ethylcarbodiimide hydrochloride (EDC.HCl), bovine serum albumin (pH 6-7) and 4-Dimethylaminopyridine (DMAP) were purchased from Spectrochem Ltd. (Mumbai, India). All other chemicals and reagents were of analytical grade and used as obtained. MIN-6 cells were procured from NCCS, Pune (INDIA).

2.2. Synthesis and characterization of LSF-LA conjugate

It was synthesized by carbodiimide coupling reaction using EDC.HCl and DMAP as shown in reaction scheme (**Figure 4.1**). Under N_2 atmosphere, LA (21.6 mmol, 1.2 eq) solution in

anhydrous CH_2Cl_2 (DCM; 250 mL; LR grade) was mixed with DMAP (21.6 mmol, 1.2 eq) for 15 min. EDC.HCl (27 mmol, 1.5 eq) solution in DCM was added and the reaction mixture was stirred for 1 h at 4 ℃. Thereafter, LSF (19.8 mmol, 1.1 eq) was added and reaction was continued for 36 h at room temperature (RT) in dark conditions. Reaction was monitored by thin layer chromatography (TLC) (mobile phase: ethyl acetate: hexane (95:05 % v/v). On completion of the reaction, reaction mixture was diluted with DCM (250 mL), washed with water (3 × 300 mL) followed by saturated sodium chloride (NaCl) solution (400 mL) and organic layer was filtered and dried on anhydrous $MgSO_4$ and evaporated under reduced pressure. The semi-solid crude product so obtained was purified using flash chromatography (normal phase flash column, Agela, Claricep^{TM}, Si 230-400 mesh) using ethyl acetate and hexane as solvent system. This yielded the final product, LSF-LA conjugate; which appeared as a transparent viscous colorless liquid. LSF-LA conjugate so obtained was characterized for its structure, molecular weight and purity by various techniques like ^{1}H NMR, ^{13}C NMR, HR-MS, FT-IR and DSC. Purity of the final product (LSF-LA) was confirmed by HPLC, using the following chromatographic conditions:-

- Column: Inertsil® ODS C18 (250×4.6 mm, 5µm)
- Mobile phase- ACN: Sodium acetate buffer (10mM; pH 4.0) (95:05 %v/v); Flow rate: 1 mL/min; Detection wavelength: 274 nm; Retention time: 18.9 min.

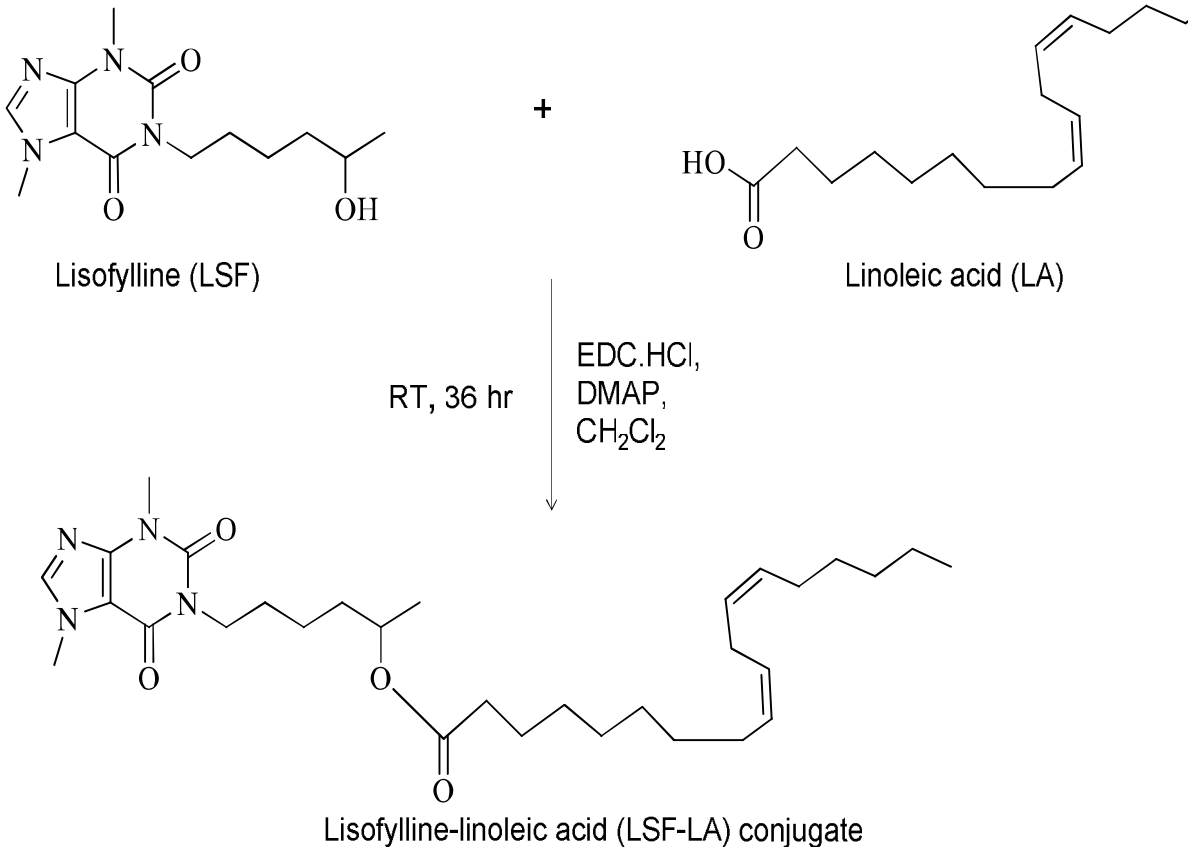

Figure 4.1. Synthetic scheme for LSF-LA conjugate

2.3. In vitro release of LSF-LA from the LSF-LA conjugate in plasma

The objective of this study was to determine stability as well as rate at which LSF-LA conjugate gets hydrolysed in plasma by cleavage of ester bond to release free LSF. LSF-LA conjugate solution (20 mg/mL in DMSO, 10 µL) was added to 1 mL of rat plasma. Samples were kept at 37 ℃ for 72 h. At pre-determined time points, 100 µL of plasma sample was withdrawn to which 50 µL of internal standard (IBMX, 2 µg/mL) solution and 2 mL of DCM were immediately added. The resulting mixture was centrifuged at 3500 rpm for 15 min at 4 ℃, after which the supernatant was transferred into a fresh tube and evaporated to dryness under nitrogen stream.

Dried samples were reconstituted in 100 µL of mobile phase and analysed by HPLC using our previously reported method.[11]

The release of LSF from LSF-LA was also carried out in PBS (pH 7.4) containing 2% w/v ethanol and 5% w/v tween 80 using a semipermeable membrane (dialysis bag, MWCO 3.5 k). Samples were kept at 37 ℃ for 72 h. At pre-determined time points, 5 mL of sample was withdrawn (5 mL media replaced), diluted with acetonitrile, centrifuged and supernatants were analysed using HPLC.

2.4. Self-assembly of LSF-LA conjugate

The amphiphilic nature of LSF-LA conjugate indicates the possibility of its self-assembly into micelles. To explore this, DCM solution of LSF-LA conjugate was added dropwise into water, followed by stirring for 15 min and evaporation of DCM. Resulting micelle formulation was sonicated for 3 min under cold conditions. The size and zeta-potential of the micelles were measured using a Zetasizer Nano-ZS (Malvern Instrument Ltd., UK) with a helium laser at 633 nm and the scattering angle was fixed at 173°. These LSF-LA self-assembled micelles shall be referred as LSF-LA SM henceforth in the text.

2.5. Critical micellar concentration (CMC) of LSF-LA conjugate

Formation of self-assembled micelles was confirmed by determination of CMC of LSF-LA conjugate in aqueous solution by fluorescence spectroscopy using pyrene as a fluorescent extrinsic probe. The self-assembled micelles of LSF-LA conjugate with a concentration of 2 mg/mL (stock solution) and pyrene (6 x 10^{-7} M) were prepared. Various dilutions of micellar solutions ranging from 1.0 × 10^{-5} mg/ mL to 2.0 mg/mL were mixed with pyrene solution and incubated for 24 h with shaking at RT. The fluorescence intensity of the solution was recorded at RT using spectrofluorimeter (RF-8201 Shimadzu, Japan) at an excitation wavelength of 300-360

nm and emission wavelength of 390 nm. To obtain the value of CMC of LSF-LA conjugate, a plot was constructed between I_3/I_1 versus logarithm of LSF-LA conjugate concentration wherein, the I_3 and I_1 values were determined from the shifting of peak intensities at the wavelengths of 337 nm and 333 nm.

2.6. Micelle aggregation number (N_{agg}) by fluorescence quenching method

The micellar N_{agg} was determined by steady state fluorescence measurements. Pyrene and cetylpyridinium chloride (CPC) were used as probe and quencher, respectively. According to the theory by Turro and Yekta,[12] the relation between the steady state fluorescence intensities with and without quencher (F_Q and F_0 respectively) is determined by the micelle concentration (M) and the quencher concentration in the micelles (Q) according to following **Equation 1 and 2**:

$$\ln\left(\frac{F_0}{F_Q}\right) = \frac{Q}{M} \qquad \textbf{Equation 1}$$

$$\text{where } M = \frac{C\text{-}CMC}{N_{agg}} \qquad \textbf{Equation 2}$$

where C = total surfactant concentration, CMC = critical micelle concentration, and N_{agg} = aggregation number.

For sample preparation, stock solutions of pyrene in LSF-LA SM solution at 30 times the CMC (Solution I) and pyrene + CPC at 30 times the CMC (Solution II) were prepared. Solution-I was prepared by transfering of 2 mL of pyrene in ethanol (10^{-4} M) into a 100 mL glass bottle followed by evaporation of the solvent under nitrogen. 100 mL of the LSF-LA micelle solution at 30 times the CMC was added to pyrene and stirred overnight to obtain the final pyrene concentration of 2×10^{-6} M. For preparing Solution II, 220.01 mg of CPC was dissolved in 20 mL of solution-I to obtain solution-II having concentration of 2.8×10^{-2} M of what? Pyrene or CPC. Appropriate volumes of these two solutions were then mixed to vary the CPC concentration from 0 to 1.54×10^{-3} M. Fluorescence steady state measurements were carried out with a Shimadzu

RF-5301 spectrofluorimeter at room temperature with an excitation wavelength of 318 nm, bandwidth 5 nm, and emission recorded from 320 nm to 450 nm. Each spectrum obtained with the instrument exhibited three vibronic peaks wherein the height (in arbitrary units) of the first vibronic peak at 376 nm considered as the fluorescence intensity of the above solutions.

2.7. Protein interaction studies with LSF and LSF-LA SM

Interaction between LSF-LA SM and serum protein was studied by fluorescence quenching method. There are the various types of fluorescence quenching, such as static, dynamic (collision) and energy transfer quenching. To determine the type of fluorescence quenching, the difference in the absorption spectra of protein and absorption spectra of protein complex with LSF-LA SM were measured.[13] BSA has been used in this study as a model protein due to its high structural homology with human serum albumin, the major soluble protein constituent of the circulatory system.[14] In fluorescence quenching method, we evaluated the change in emission fluorescence of BSA after incubation of BSA with LSF-LA SM. Apart from the binding constant, the number of binding sites per BSA molecule were also determined. For sample preparation, a series of stock solutions (in water) of LSF-LA SM in the range of 0–100 μM were prepared where BSA concentration was kept constant (2 μM). Incubation time for protein and drug solution mixture was kept for 30 min. Fluorescence measurements were performed by Shimadzu RF-5301spectrofluorimeter using 5-nm excitation and emission slit width. The samples were scanned in the range of 290–450 nm, and the fluorescence intensity at 343 nm was determined with excitation at 280 nm. LSF in similar concentration range was used as control. After 30 min of incubation, particle size measurement was carried out for BSA (fixed 2 μM) and/or LSF-LA SM (0-100 μM) and BSA mixture.

The fluorescence quenching data was plotted as log $(F_0\text{-}F_Q)/F_Q$ against log of quencher concentration (LSF-LA SM or LSF; log [Q]), with F_Q and F_0 representing the fluorescence

intensity in the presence and absence of quencher, respectively. When small molecules bind independently to a set of equivalent sites on a molecule, the equilibrium between free and bound molecules is represented by the following Scatchard **Equation 3**,[15,16]

$$\log \frac{F_0 - F_Q}{F_Q} = \log K_b + n. \log [Q] \qquad \textbf{Equation 3}$$

where K_b is the apparent binding constant and *n* is the number of binding sites per BSA molecule.

For all samples, the absorption spectra were also recorded using an ultraviolet–visible (UV–vis) V-650 Jasco spectrophotometer equipped with a quartz cell with 1-cm path length to determine the possible mechanism of protein-LSF-LA SM interaction.

2.8. In vitro efficacy studies of LSF-LA SM

To evaluate the efficacy of LSF-LA SM in diabetic conditions, mouse insulinoma cells, MIN-6 were used. Cells were grown in RPMI media supplemented with 10% FBS and 1% antibiotic solution and incubated at 5% CO_2 and 37°C. For treatments, LSF-LA and LA were dissolved in cell culture grade DMSO and the highest used concentration of DMSO was kept as control (0.1% v/v).

2.8.1. Cell viability assay

The aim of this experiment was to determine if LSF-LA SM induce any toxicity in the insulinoma cells. MIN6 cells (5×10^3/well) were seeded in a 96 well cell culture plate and allowed to adhere for 24 h. Three different concentrations of LSF-LA conjugate ranging from 10-40 μM were added to the cells and incubated at 37℃/5% CO_2 for 48 h. Untreated cells and cells treated with free LSF and LA at equivalent concentrations to LSF-LA conjugate were kept as controls. After 48h, MTT assay was performed and optical density (OD) was recorded at 560 nm and 630 nm as reference wavelength. The percentage cell inhibition was determined by comparison with untreated cells. (**Equation 4**)

% Cell viability = (OD samples wells/OD control wells) × 100 **Equation 4**

2.8.2. Protective effect rendered by LSF-LA SM to cells under inflammatory conditions

To evaluate if conjugation of LSF with LA has affected the protective role of LSF on β–cells under inflammatory conditions, these experiments were carried out. MIN6 cells were seeded in 96 well cell culture plates (5×10^3 cells/well) and allowed to adhere for 24 h. Thereafter, the cells were exposed to a cocktail of pro-inflammatory cytokines (TNF-α; 10 ng/mL, IL-1β; 5 ng/mL and IFN-γ; 100 ng/mL) to induce inflammation.[7] To these cells, along with cytokines, free LSF, free LA and LSF-LA conjugate were also added (~20 μM) and incubated for 48 h. Thereafter, the cells were evaluated for their viability by MTT assay and insulin secreting ability, using a static incubation method wherein, MIN-6 cells exposed to inflammatory cytokine cocktail and drug were sequentially incubated in the media containing basal (3.33 mM) and stimulatory glucose (33.33 mM) concentrations at 37 ºC for 1 h each. The basal and stimulatory glucose solutions were prepared in Krebs-Ringer bicarbonate HEPES buffer (pH 7.4). Supernatants were collected and analyzed for insulin content using commercially available ELISA kit (Crystal Chem, USA).

2.8.3. Suppression of PBMC proliferation and activation by LSF-LA SM

The effect of LSF and LSF-LA SM on proliferation of PBMCs under PHA stimulated conditions was studied. PBMCs were freshly isolated from mouse blood using Ficoll-Paque density gradient method. These cells were then exposed to PHA (1μg/mL, mitogen activator) in the presence of LSF-LA SM for 48 h keeping suitable controls as PBMCs with PHA (1μg/ml) alone, with PHA and free LSF and with PHA and free LA. After 48 h of incubation, the supernatants were evaluated for PBMCs proliferation by CFSC staining assay and for production of inflammatory cytokines viz. IFN-γ and TNF-α. For CFSE staining, the freshly isolated PBMCs were incubated with staining solution containing CFSE for 30 min at 5% CO_2/ 37ºC in an

incubator. The cell-CFSE mixture was occasionally inverted to ensure mixing of the dye with the cells and protected from light. After 30 min, the cells were centrifuged at 1250 rpm for 5 min and washed twice with PBS, recounted and used for the experiment (as detailed above).[17] After 48 h of incubation, the proliferation of CFSE stained PBMCs was studied using flow cytometry with a 488 nm excitation laser. The extent of cell activation was also determined by measuring the level of inflammatory cytokines, TNF-α and IFN-γ in the conditioned medium of PBMCs using ELISA kits.

2.8.4. Cellular uptake study by HPLC

MIN6 cells were cultured with LSF (20 μM) and LSF-LA SM (~20 μM to LSF) for 6 h, along with suitable controls. After digesting with trypsin, the cell suspension was drawn and centrifuged at 1000 rcf/min for 10 min, to separate the cells and culture medium. For extraction, 50 μL of I.S (IBMX) and 1.2 mL of DCM were added to the 0.5 mL of sample medium followed by centrifugation of 3500 rpm for 15 min, 1 mL of DCM layer was collected and dried. After 100 μL of reconstitution with mobile phase, 80 μL of sample was injected in HPLC for LSF and LSF-LA analysis.

2.9. In vivo studies for LSF-LA SM

Animal experiment protocol was approved by IAEC, BITS-PILANI (IAEC/RES/19/07/Rev-1/21/8), Pilani and all experiments were conducted as per CPCSEA guidelines. Rats were housed in well ventilated cages at standard laboratory conditions with regular light/dark cycles for 12 h and fed with standard normal diet *ab libitum.*

2.9.1. PK studies of LSF and LSF-LA SM

The PK studies of LSF and LSF-LA SM were performed on Wistar rats (200-220 g). LSF and LSF-LA SM were administered intravenously at the dose of 25 mg/kg and 50 mg/kg

(equivalent to 25 mg/kg of free LSF) respectively with maximum dosing volume of 250 µL to each rat without fasting (n=4). After i.v dosing, blood samples were collected at each of the preset time points, 5, 15, 30, 45 min, 1, 2, 3, 4, 6, 8, 12, 24 and 36 h. LSF and LSF-LA conjugate plasma concentration-time profiles were plotted and analyzed by non-compartmental model using Phoenix 2.1 WinNonlin (Pharsight corporation, USA) to determine elimination half-life ($t_{1/2}$); drug concentration in plasma at t=0 (C_0); area under curve from zero to the last time point (AUC_{0-t}); area under curve from zero to infinity ($AUC_{0-\infty}$); mean residence time (MRT); clearance (CL) and, apparent volume of distribution (V_z). Since LSF is known to interconvert to PTX, plasma levels of PTX in both LSF and LSF-LA conjugate were also assessed.

2.9.2. In vivo efficacy studies in STZ induced T1DM model

Diabetes was induced in the male Wistar rats weighing 180-220 g. Animals were injected with a single high dose of STZ (55 mg/kg, i.p.) dissolved in sodium citrate buffer (0.01 M, pH 4.5) while the respective control rats received the vehicle, citrate buffer (pH 4.5). After 72 h of STZ injection, fasting glucose levels were measured, animals showing plasma glucose levels >250 mg/dl were considered diabetic. Animals were randomly divided into different groups, namely non-diabetic control (NC), diabetic control (DC), diabetic/treated with free LSF and diabetic/treated with self-assembled micelles of LSF-LA.

Treatment was started after 3rd day after confirming the diabetic conditions. For treatment, free LSF was administered as solution prepared in water for injection at two different doses, 25 mg/kg, i.p. twice daily and 15 mg/kg, i.p. once daily. LSF-LA conjugate was self-assembled into micelles using water for injection and administered at a dose of 30 mg/kg (~ 15 mg/kg of free LSF) i.p. once daily. Treatment was continued for 1 week.

2.9.3. Fasting glucose, insulin and cytokines levels

Fasting glucose levels were measured daily by tail bleeding method using Accu-Check active glucometer. After 7 days, the levels of insulin and inflammatory cytokines, TNF-α and IFN-γ in plasma were also measured using ELISA kits.

2.9.4. Histopathology and immunohistochemical analysis

After 1 week of treatment, animals were euthanized and pancreata were isolated and fixed in 10% paraformaldehyde. Tissues were then processed for paraffin embedding, subsequent serial sectioning, and stained with hematoxylin/eosin (H&E) to allow the assessment of pancreatic islet morphology in the studied groups. For immunohistochemical (IHC) analysis of insulin, same pancreatic tissue samples were used for each of the groups (as used for H&E), IHC was performed using the peroxidase/anti-peroxidase method. Nonspecific peroxidase reactions were blocked with methanol containing 0.1% H_2O_2 and the sections were also incubated with normal goat serum to avoid nonspecific reactions with the background once the samples were incubated with the specific antibody against insulin (Insulin rabbit IgG, dilution 1:2,000; Santa Cruz Biotechnology, Santa Cruz, CA, USA). The sections were then washed with a phosphate-buffered saline (PBS) and incubated with a secondary antibody (goat anti-rabbit IgG, dilution, 1:2,000; Sigma), before being washed in PBS again and, finally, incubated with the peroxidase/anti-peroxidase complex (dilution, 1:200). The peroxidase reaction was carried out using a solution of 3,3′-diaminobenzidine tetrahydrochloride containing 0.01% H_2O_2 in Tris–HCl buffer (0.05 M, pH 7.6). After immunostaining, the sections were lightly counterstained with hematoxylin and observed under a light microscope. For determining the % insulin staining area (brownish stain), six random pancreatic islets in each group were selected in the images and quantified for insulin staining area by using ImageJ software (version 1.42q, NIH, USA).

2.10. Statistical analysis

Statistical analysis was performed using one way ANOVA followed by Tukey–Kramer multiple comparison post-test using graphpad prism (Version 6.01) software.

3. Results

3.1. Synthesis and characterization of LSF-LA conjugate

Figure 4.2A and B show the ^{1}H and ^{13}C NMR spectra of LSF-LA conjugate along with free LSF and LA. Comparing the ^{1}H NMR spectrum of LSF-LA conjugate with that of LSF, the peak at 3.75 ppm (f) related to hydroxyl proton present in side chain of LSF (which is the only conjugation site available in LSF) disappears completely in LSF-LA conjugate. It indicates that –CH-OH group of LSF has been consumed in ester bond formation between LSF and LA. This was confirmed by the presence of a new peak at chemical shift value at 4.9 ppm (-CH-COO; f') in LSF-LA conjugate NMR spectrum. This chemical shift can be attributed to strong π-π stacking after esterification. Since ^{1}H NMR was unable to confirm the presence or absence of free LA in LSF-LA conjugate, additionally ^{13}C NMR was performed. ^{13}C NMR spectrum of LA exhibited the carbon signal at 180 ppm corresponding to its terminal -COOH which disappeared in LSF-LA conjugate as shown in **Figure 4.2B (ii)**. Moreover, LSF-LA conjugate showed the carbon signal at 174.06 ppm in the ^{13}C NMR spectrum corresponding to its –COO- group.

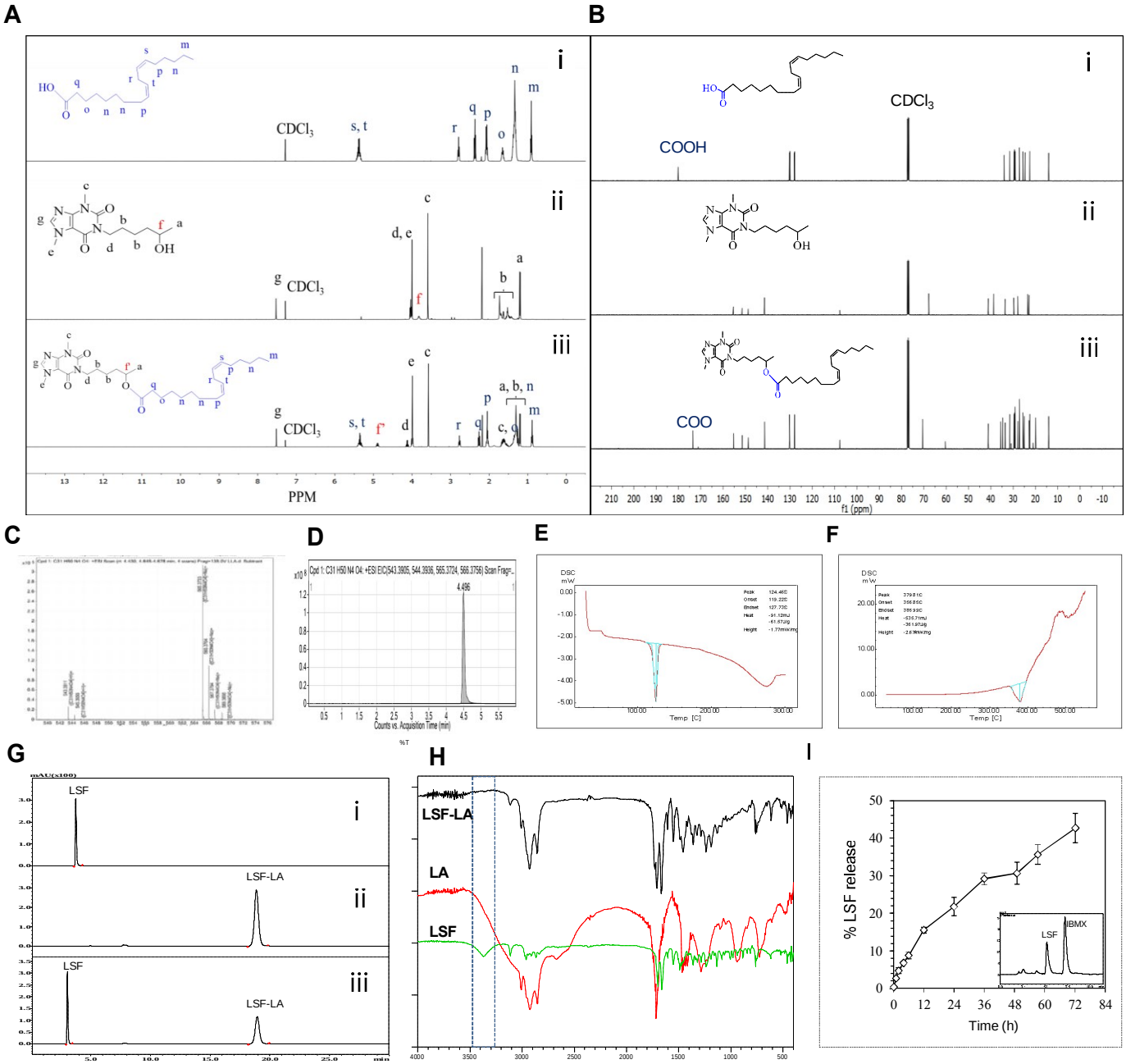

Figure 4.2. Characterization of LSF-LA conjugate. (A) ^{1}H NMR and (B) ^{13}C NMR, here (i) represents LA alone, (ii) corresponds to LSF alone and, (iii) corresponds to LSF-LA conjugate, (C) HR-MS analysis (M+H)+ = 543.3911, mass = 542.3822 g/mol and, (D) LC chromatogram obtained from HR-MS; DSC analysis for melting point determination of (E) LSF and (F) LSF-LA conjugate (G) HPLC analysis for purity determination, (H) FT-IR and, (I) *in-vitro* release of LSF from LSF-LA SM in rat plasma and representative chromatogram for 1 h sample.

For determination of molecular weight of LSF-LA conjugate, HR-MS analysis was carried out (**Figure 4.2C and D)**. Expected mass for LSF-LA conjugate by its molecular formula ($C_{13}H_{50}N_4O_4$) was calculated to be 542.3832 g/mol. Mass analysis was carried out in ESI+ mode wherein, $(M+H)^+$ ion peak was observed at m/z 543.3911 (**Figure 4.2C**). Thus, the mass of LSF-LA as calculated by HR-MS is 542.3832 g/mol (M, 543.3911-1.0078 (Mass of ^1H) =542.3832). No interfering peak of LSF was observed in LC chromatogram (**Figure 4.2D**) of LSF-LA conjugate.

Further, DSC revealed a change in the melting point (**Figure 4.2E and F**) of LSF-LA conjugate (379.81℃) as compared to the melting point of LSF alone (124.45℃). Again, there was no melting peak corresponding to free LSF present in LSF-LA conjugate thermogram.

HPLC analysis of LSF-LA conjugate and LSF revealed that the retention time of LSF-LA increased to 18.9 min as compared to LSF which eluted out at 3.1 min, indicating a significant increase in hydrophobicity of LSF upon attaching LA (**Figure 4.2G).** Further, LSF-LA conjugate showed no peak at 3.1 min, confirming the absence of any unreacted LSF as impurity as previously also indicated by ^1H NMR. Peak purity of LSF-LA conjugate was also analyzed and was found to be >98%. In **Figure 4.2G (iii)**, free LSF and LSF-LA conjugate were mixed in 1:1 ratio and the peak area observed for LSF-LA conjugate was half that of free LSF, confirming successful conjugation of LSF and LA in 1:1 ratio and absence of free LSF.

FTIR spectrum of LSF-LA conjugate also confirmed successful conjugation. Functional group region 4000-1400 cm^{-1} in FT-IR showed –CH-OH peak at 3400-3300 cm^{-1} (**Figure 4.2H**), which was absent in LSF-LA conjugate as free –CH-OH group of LSF participated in ester bond formation with -CH-COOH group of LA. All experimental results demonstrated that LSF-LA conjugate was synthesized successfully.

3.2. In vitro release of LSF-LA from the LSF-LA conjugate in plasma

As shown in **Figure 4.2I**, LSF-LA conjugate gets slowly hydrolyzed in rat plasma. During the first 2 h, only 4.7 % of free LSF is released followed by release of 42.73% LSF from LSF-LA within the next 72 h. It is evident from this experiment that the designed LSF-LA conjugate is hydrolysable in rat plasma and is able to release free LSF in a sustained manner to elicit its therapeutic effect.

The release study of LSF from LSF-LA conjugate in PBS (pH 7.4) containing 2% w/v ethanol and 5% w/v tween 80 showed a negligible release of LSF which might be attributed to the stability of the conjugate (resistance to hydrolysis) in the release media.

3.3. Self-assembly and CMC of LSF-LA SM

LSF-LA conjugate contains hydrophobic (LA) and hydrophilic (LSF) components in 1:1 proportion that provides it a characteristic ability to self-assemble into micelles in water. **Figure 4.3A** gives the dynamic light scattering (DLS) curve of LSF-LA micelles in aqueous medium at a concentration of 0.5 mg/mL, indicating the formation of micelles with a unimodal distribution and an average hydrodynamic diameter of 156.9 nm (polydispersity index: 0.187). The zeta potential of the LSF-LA conjugate micelles was negative (-17.0 ± 4.04 mV, **Figure 4.3B**). As shown in **Figure 4.3C**, CMC value for LSF-LA conjugate was found to be 1 μg/mL indicating micelle formation and hence its ability to self-assemble.

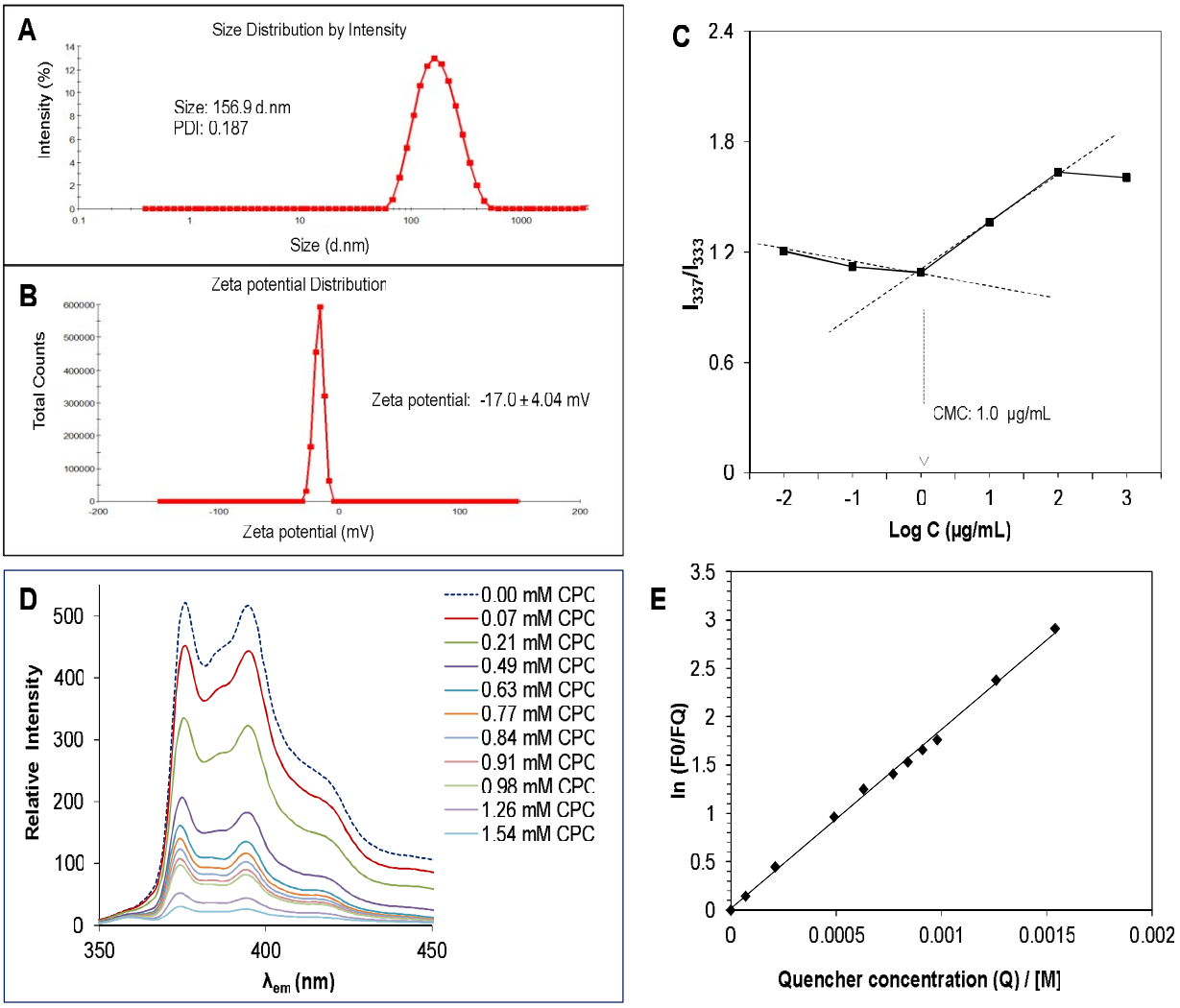

Figure 4.3. Self-assembled micelles of LSF-LA conjugate, (A) Particle size distribution, (B) zeta-potential curve and, (C) CMC determination (D) steady-state emission spectra of pyrene in LSF-LA SM (30 folds CMC) at different CPC concentrations (E) plot of $\ln(F_0/F_Q)$ against quencher concentration for LSF-LA SM (30 folds CMC) at room temperature. *CPC: Cetylpyridinium chloride

3.4. Micelle Aggregation number (N_{agg}) by fluorescence quenching method

The aggregation number of LSF-LA self-assembled micelles was obtained from the static fluorescence quenching. **Figure 4.3D** showed decrease in pyrene emission in the presence of different quencher (CPC) concentrations at 30 times the CMC of LSF-LA SM. **Figure 4.3E** shows

plot of $\ln(F_0/F_Q)$ vs. Q. It can be seen that straight line can be drawn through origin. The inverse of the slope corresponds to the micellar concentration [M], and then the aggregation number could be obtained using **Equation 2.** N_{agg} for LSF-LA self-assembled micelle was found to be 54.

3.5. Protein interaction studies with LSF and LSF-LA SM

In this study, the interactions between, BSA-(LSF-LA SM) and BSA-LSF were investigated by fluorescence quenching. **Figure 4.4A** shows emission spectra of BSA-LSF-LA SM and **Figure 4.4B** shows BSA-LSF interaction. There was no change in the wavelengths at which fluorescence peaks were observed, whereas fluorescence intensities of BSA decrease as the concentration of LSF or LSF-LA micelles increase. As shown in **Figure 4.4**, LSF-LA micelles or LSF exhibited no fluorescence emission in the range of these wavelengths as seen in the respective graph (Plot (I) for LSF-LA micelles in **Figure 4.4A** and plot (H) for free LSF in **Figure 4.4B**). This indicates that there were interactions between LSF or LSF-LA micelles and BSA. Further, **Figure 4.4C** shows a plot of $\log (F_0\text{-}F_Q)/F_Q$ vs. log [Q]. According to **Eq.III**, K_b and *n* values were determined using intercept and slope respectively. K_b for LSF-LA micelles and LSF was found to be 2.14×10^4 and 6.11×10^4 $L.mol^{-1}$ respectively. The value of *n* was calculated from the slope of respective graphs and was determined to be 1.11 and 1.16 per BSA molecule for LSF-LA micelles and LSF respectively.

During dynamic quenching, the UV–vis absorption spectrum of the fluorophore does not change; only the excited-state fluorescence molecule is influenced by the quencher. However, during static quenching, a compound is formed between the ground state of the fluorophore and quencher, and the absorption spectrum changes. [13,18] Based on UV and emission spectra, a static quenching mechanism was indicated between BSA and LSF or LSF-LA SM **(Figure 4.4D).**

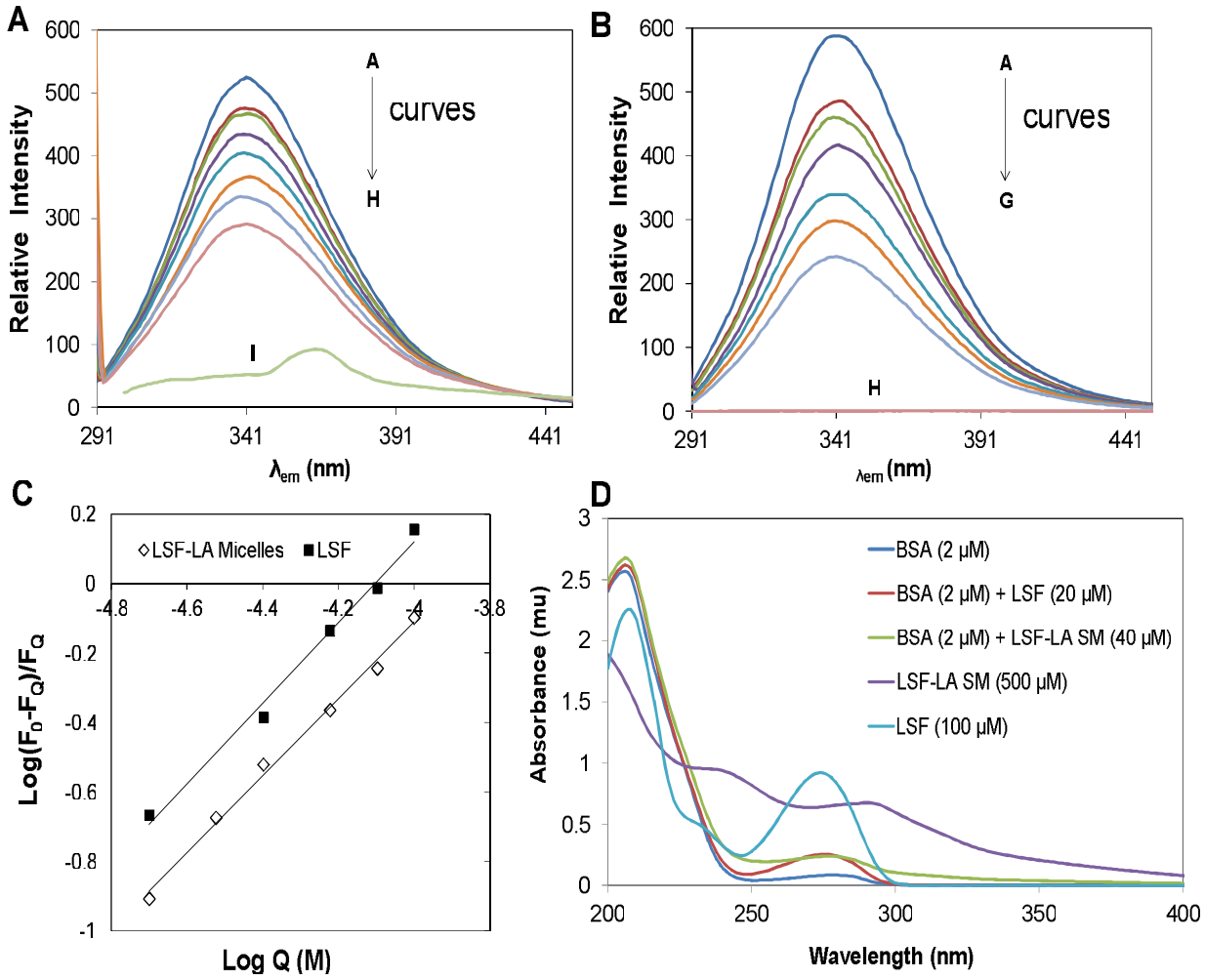

Figure 4.4. BSA-LSF interaction study. (A) Emission spectra of BSA (λ_{exc} = 280 nm) in the presence of various concentrations of LSF-LA SM. [BSA] = 2.0 μM; [LSF-LA SM] = 0.0; 10; 20; 30; 40; 60; 80; 100 μM, corresponding to curves A–H. Plot I corresponds to the emission spectrum of 500 μM LSF-LA SM alone, (B) emission spectra of BSA in the presence of various concentrations of LSF. [BSA] = 2.0 μM; [LSF] = 0.0; 20; 30; 40; 60; 80; 100 μM, corresponding to curves A–G. Plot H corresponds to the emission spectrum of 100 μM LSF alone, (C) plot of (F_0/F_Q) against quencher concentration at room temperature and, (D) absorption spectra of BSA, LSF-LA SM, LSF, and BSA with LSF or LSF-LA SM.

As shown in **Figure 4.5A and B,** an increase in particle size as well as in PDI was observed after incubating LSF-LA SM with BSA at different concentrations further confirming BSA and LSF-LA SM interaction.

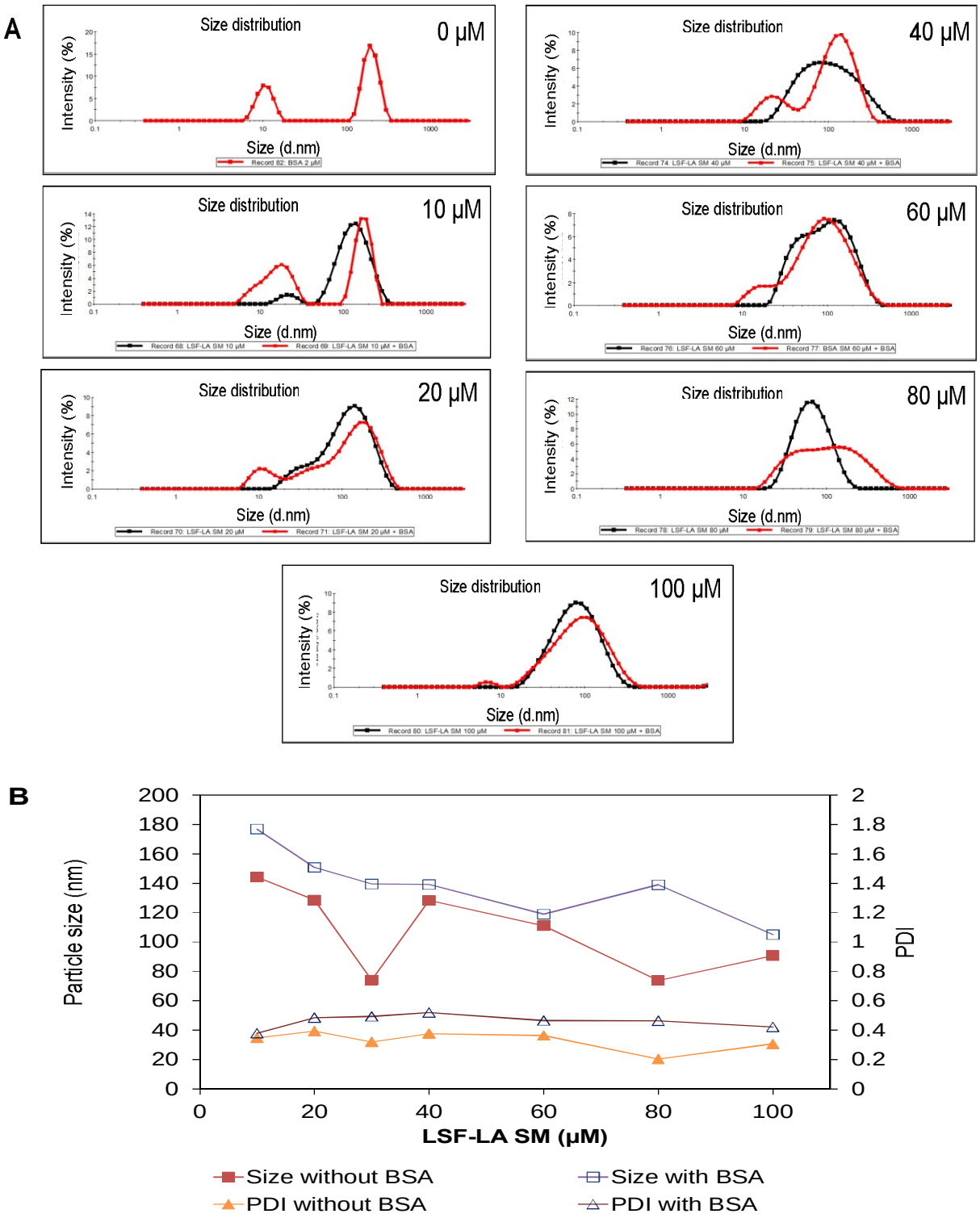

Figure 4.5 (A) Particle size distribution curves of LSF-LA SM at different concentrations (0-100 µM) with and without BSA and, (B) effect on particle size and PDI of LSF-LA SM at different concentrations (0-100 µM) in the presence and absence of BSA (2 µM).

3.6. In-vitro efficacy studies of LSF-LA conjugate

3.6.1. Cell viability assay

Cell viability assay was performed to assess the cytotoxicity of synthesized LSF-LA conjugate in MIN-6 cells at different concentrations (10, 20 and 40 μM). LSF-LA conjugate was found to be non-toxic at all the tested concentrations which indicated that the conjugate did not have any harmful effect on the cells (**Figure 4.6A**).

3.6.2. Protective effect rendered by LSF-LA conjugate to cells under inflammatory conditions

As seen in **Figure 4.6B**, in the presence of cocktail of cytokines, TNF-α, IL-1β and IFN-γ, LSF and LSF-LA conjugate rendered significant protection to β -cells. Cell viability under inflammatory conditions was reduced to ~42.92% however, presence of LSF and LSF-LA conjugate (20 μM) restored the viability to 73.55 and 83.90% respectively. LSF-LA conjugate showed a significantly higher restoration of cell viability of β -cells in comparison to free LSF. However, no significant improvement was observed in β -cell viability upon increasing the concentration of LSF and LSF-LA conjugate from 20 μM to 40 μM.

Figure 4.6C compares the amount of insulin secreted by β-cells under inflammatory conditions in response to the basal (3.33 mM) and stimulated levels of glucose (33.3 mM). As expected, cells in the presence of cytokines showed decreased level of insulin production when compared to normal cells (without cytokines). However, in the presence of LSF and LSF-LA conjugate (20 μM), insulin secretion was significantly improved under inflammatory conditions wherein, incubation with LSF-LA conjugate showed a significant increase in the levels of insulin produced by the cells in comparison to free LSF.

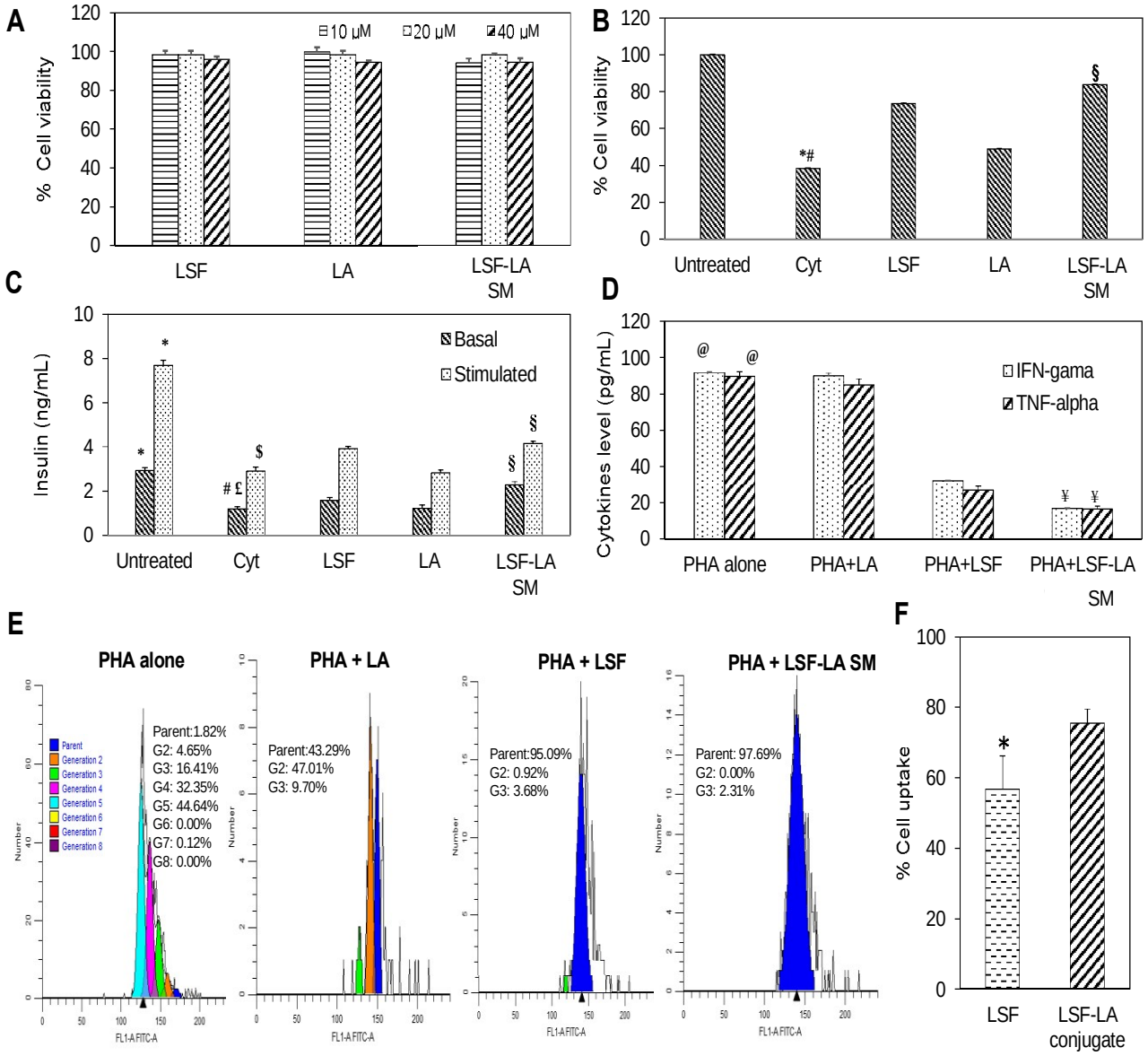

Figure 4.6. Cell culture studies of LSF-LA SM in insulin secreting MIN-6 cells. (A) Cytotoxicity, (B) anti-inflammatory activity of synthesized LSF-LA conjugate (20µM) in the presence of cytokines (TNF-α, IL-1β and IFN-γ), (C) basal and stimulated insulin levels after inflammatory challenge following treatment with LSF, LA and LSF-LA (20 µM), (D) IFN-γ and TNF-α levels in the conditioned media of PBMCs, (E) effect of LSF-LA on cell proliferation of activated PBMCs by flow cytometry and, (F) cellular uptake of LSF and LSF-LA SM (~20µM) by HPLC, *LSF vs. LSF-LA SM ($^{*}P<0.05$). *Cyt *vs.* Untreated; $^{\#}$Cyt *vs.* all; §LSF-LA *vs.* LSF and LA ($^{*\#\S}P < 0.001$) $^{@}$PHA stimulated PBMCs *vs.* LSF and LSF-LA; $^{¥}$LSF-LA *vs.* LSF ($^{@¥}P<0.001$).

3.6.3. Suppression of PBMC proliferation and activation by LSF-LA conjugate

As shown in **Figure 4.6D**, LSF-LA conjugate significantly decreased ($p< 0.001$) IFN- γ and TNF-α level in comparison to free LSF treated cells. PHA stimulated cells and those treated with LA did not exhibit any significant difference in IFN-γ and TNF-α levels. Decreased levels of inflammatory cytokines in PHA stimulated cultures signify ability of LSF-LA conjugate to impair the activation of adaptive immune system in T1DM.

Figure 4.6E showed PBMC proliferation in the presence of free LSF, free LA and LSF-LA conjugate upon stimulation by PHA. Here, each peak of the flow cytometric graph represents a cell division or generation and cells treated with PHA alone exhibit maximum proliferation (upto 7th generation) in contrast to the un-stimulated cells which do not proliferate beyond 1st generation (data not shown). In the presence of LSF and LSF-LA conjugate, a significant reduction in the proliferation of PBMCs is evident. Thus, it was confirmed that LSF and LSF-LA conjugate markedly suppressed PBMC proliferation even in the presence of a mitogen stimulator, PHA.

3.6.4. Cellular uptake study by HPLC

Figure 4.6F shows cellular uptake of free LSF and LSF-LA SM at concentration of 20μM and 40 μM (~20 μM) respectively. In comparison to free LSF group (56.86 ± 9.26), LSF-LA SM (75.48 ± 4.01) showed higher cellular uptake because of its hydrophobicity and nano structure.

3.7. In-vivo studies of LSF-LA conjugate

3.7.1. PK studies of LSF and LSF-LA conjugate

As shown in **Table 4.1**, LSF-LA conjugate significantly improved the PK profile of free LSF. LSF-LA conjugate showed half-life of 3.82 ± 0.13 h which was 5.7 folds higher than that of free LSF (0.661 ± 0.03 h). Thus, LSF-LA conjugate also increased MRT of LSF (0.93 to 4.78

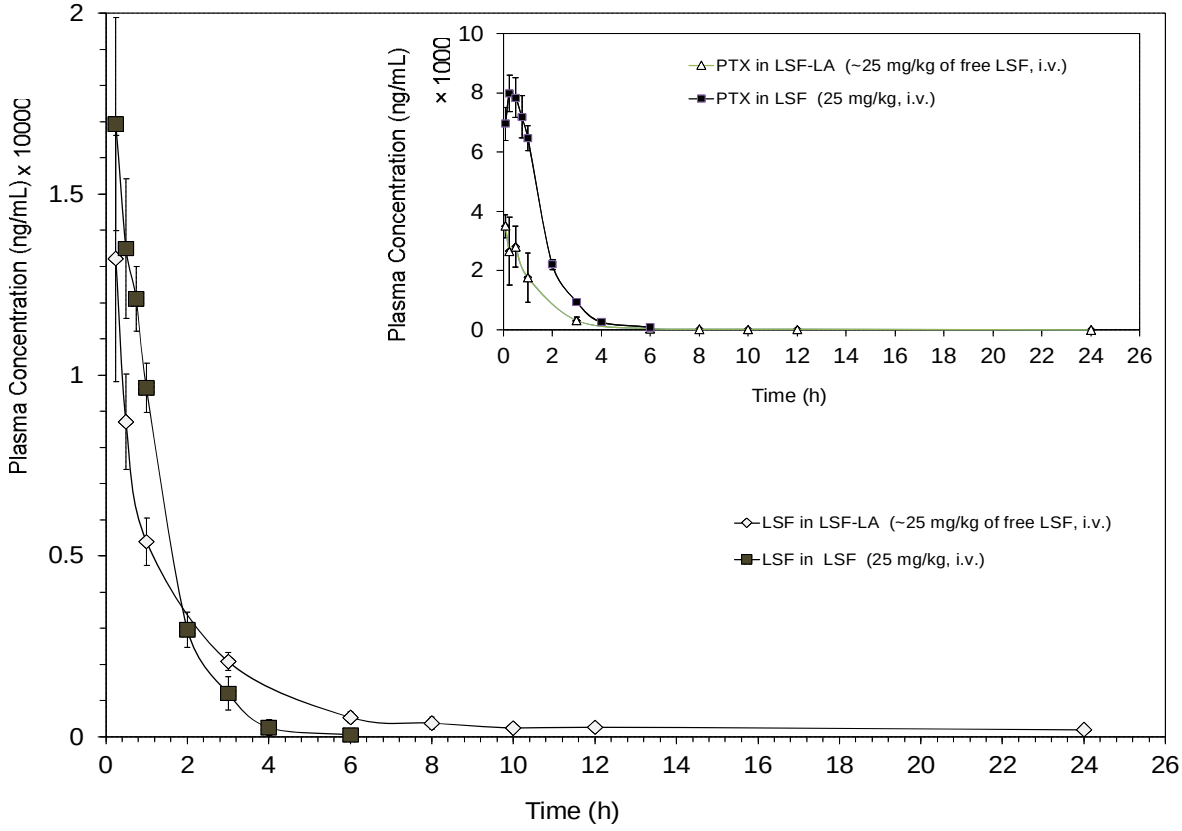

Figure 4.7. Pharmacokinetic studies of free LSF and LSF-LA conjugate after intravenous (i.v.) administration in rat at a dose of ~25 mg/kg of free LSF. Due to interconversion of LSF to PTX, PTX levels were also observed in the plasma; PTX plasma concentration-time profiles obtained after administration of free LSF and LSF-LA conjugate are also shown as inset. Each point represents mean (n=4) ± SEM.

h). An increase in MRT indicated the probability of a prolonged therapeutic action and hence reduced dosing of LSF, which was later confirmed by pharmacodynamic studies in diabetic animals. LSF-LA conjugate showed 5 times higher apparent volume of distribution (5279.41± 377.18 mL/kg) compared to free LSF (997.077 ± 71.35 mL/kg) indicating that LSF-LA conjugate was widely distributed to different tissues. In comparison to free drug, clearance of LSF-LA conjugate was found to be 955.08 ± 35.36 mL/h/kg, which was lesser in comparison to that of free LSF (1044.124 ± 43.53 mL/h/kg). PTX was also detected in the plasma upon administration of

both free LSF and LSF-LA conjugate attributed to the well reported LSF-PTX *in vivo* interconversion.[6] As shown in **Figure 4.7**, a significant decrease in PTX plasma level (~50 %) was

Table 4.1
The non-compartmental pharmacokinetic parameters for LSF and LSF-LA SM in rat plasma after i.v. bolus at dose of 25 mg/kg LSF and 50 mg/kg of LSF-LA (~25 mg/kg to LSF)

Parameters	Mean ± SEM	
	Free LSF (n=4)	**LSF in LSF-LA (n=4)**
C_o (ng/mL)	22295.204 ± 3691.39	20110.94± 2552.43
$t_{1/2}$ (h)	**0.661 ± 0.03**	**3.82 ± 0.13**
Ke (1/h)	1.056 ± 0.05	0.18 ± 0.01
$AUC_{0\text{-last}}$ (ng.h/mL)	23944.589 ± 992.83	25177.93 ± 1037.94
$AUC_{0\text{-}\infty}$ (ng.h/mL)	24067.711 ± 995.38	26245.08 ± 937.06
$AUMC_{0\text{-last}}$ (ng.h/mL)	22441.435 ± 1592.68	93378.84 ± 4459.30
$AUMC_{0\text{-}\infty}$ (ng.h/mL)	22789.458 ± 1692.67	124912.76 ± 6029.35
MRT (h)	**0.937 ± 0.07**	**4.78 ± 0.367**
V_z (mL/kg)	**997.077 ± 71.35**	**5279.41± 377.18**
CL (mL/h/kg)	**1044.124 ± 43.53**	**955.08 ± 35.36**

observed in LSF-LA conjugate PK in comparison to LSF PK which might be attributed to a decrease in LSF-PTX *in vivo* interconversion upon administering LSF as a self-assembling conjugate instead of administering it in free form.

3.7.2. In vivo efficacy studies in STZ induced T1DM model

To evaluate whether efficient and improved PK resulted in the enhancement of therapeutic efficacy, LSF-LA conjugate was tested in STZ induced T1DM rat model over 1 week treatment period. The results were compared to free LSF administered at two dose levels that is, 25 mg/kg, twice daily and at 15 mg/kg, once daily (same dose as that of LSF-LA conjugate).

3.7.3. Fasting glucose, insulin and cytokines levels

As shown in **Figure 4.8A**, a decrease in the fasting glucose levels was seen after 7 days of LSF-LA conjugate treatment. Since day 2 of treatment, glucose levels started to decrease and this trend continued up to 7 days of treatment. Free LSF at a dose of 15 mg/kg once daily lowered glucose levels in some rats but failed to maintain the reduced levels compared to free LSF 25 mg/kg twice daily dose. LSF alone (25 mg/kg twice daily dose) stabilized blood glucose levels in some rats but did not correct the values to normal. However, upon treatment with LSF-LA SM, blood glucose levels got stabilized as well as corrected to normal level in some animals. As shown in **Figure 4.8B and D**, LSF-LA conjugate treated group showed drastic reduction in the levels of inflammatory cytokines, TNF-α and IFN-γ along with increased levels of insulin *in vivo* in comparison to free LSF treated group.

3.7.4. Histopathology and immunohistochemical analysis

The H&E-stained sections of rat pancreas of diabetic group showed a significant decrease in the number of β cells of the islets of Langerhans compared to the control group (normal animals) where large number of β cells (seen as H&E-stained blue cells) were seen distributed throughout the islet (**Figure 4.8C (I)**). The damage or necrosis of β cells in diabetic control group is a hallmark of diabetes. In free LSF (25 mg/kg, twice daily) and LSF-LA (15 mg/kg, once daily) conjugate treated groups, more number of β cells were observed as compared to the diabetic control group. The infiltration of inflammatory immune cells to islets was much lesser in LSF-LA treated group compared to the diabetic control group. Although the rats treated with free LSF at 25 mg/kg (twice daily) dose showed better β cell protection compared to LSF at 15 mg/kg (once daily) dose, the distorted morphology of the islets in both the groups was similar to the un-treated diabetic group (DC) group. As shown in **Figure 4.8C (II)** IHC for insulin in the non-diabetic (normal control) rats revealed presence of abundant insulin (% insulin staining area,

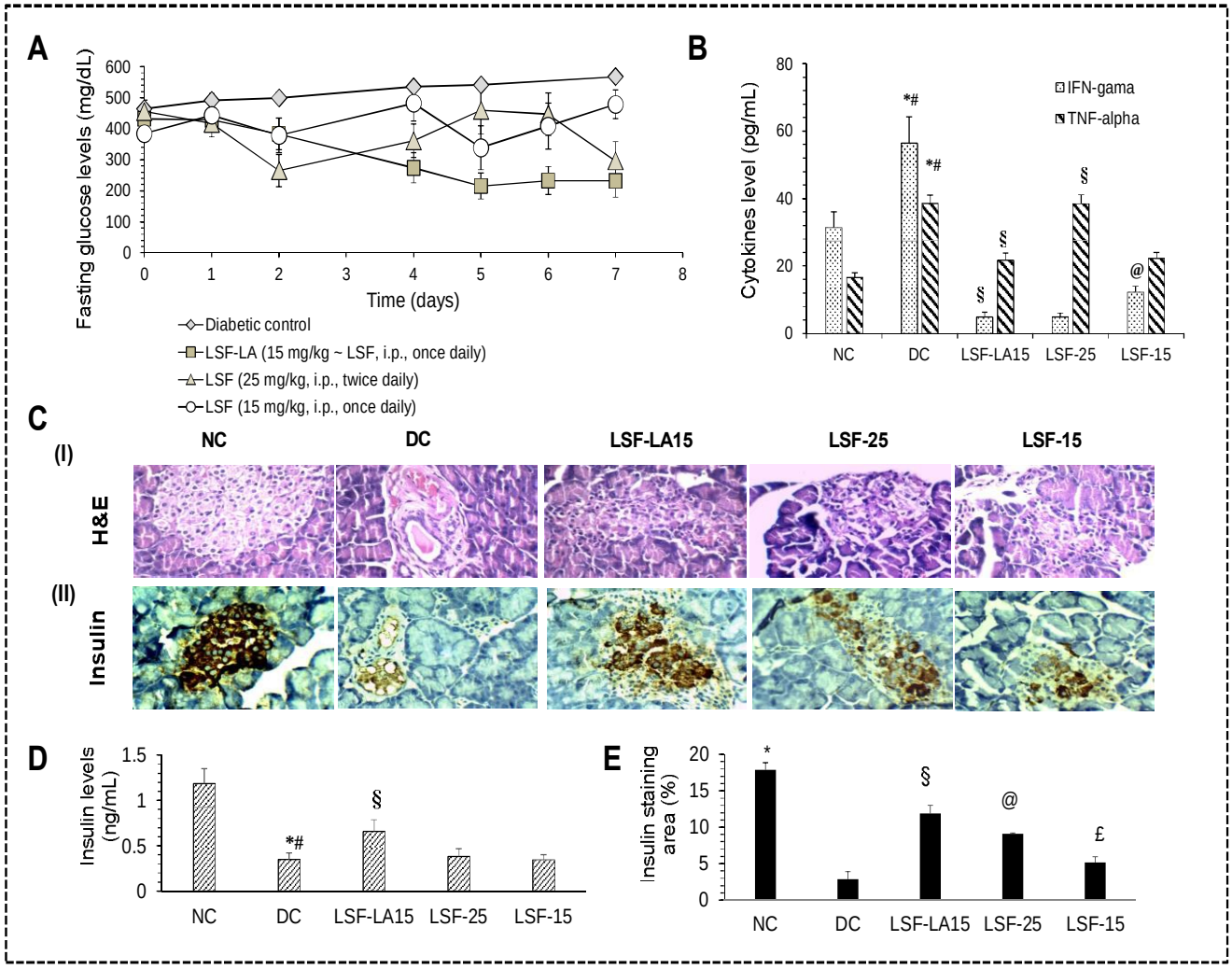

Figure 4.8. *In vivo* efficacy study of LSF-LA SM in STZ induced T1D animal model. (A) Fasting blood glucose levels, (B) IFN-γ and TNF-α levels in rat plasma after 1 week of treatment. *NC *vs.* DC; $^{\#}$DC *vs.* all groups; §LSF-LA15 *vs.* LSF-25 and LSF-15; $^{@}$LSF-15 *vs.* LSF-LA15 and LSF-25 ($^{*\#\S}P<0.001$; $^{@}P<0.05$) *NC *vs.* DC; $^{\#}$DC vs. LSF-LA15 and LSF-15; §LSF-LA15 *vs.* LSF-25; §LSF-25 *vs.* LSF-15 ($^{*\#\S\S}P<0.001$), (C) immunohistochemical (IHC) analysis of pancreatic tissues (I) H&E and (II) insulin staining (magnification ×400, scale: 50 µm), (D) insulin levels in rat plasma after 1 week of treatment. *NC *vs.* DC; $^{\#}$DC *vs.* LSF-LA15; §LSF-LA15 *vs.* LSF-15 ($^{*}P<0.001$; $^{\#\S}P<0.05$) and, (E) in IHC, % insulin staining area analyzed by ImageJ software. *NC *vs.* all groups; §LSF-LA15 *vs.* DC and LSF-15; $^{@}$LSF-25 *vs.* LSF-LA15; $^{£}$LSF-15 *vs.* LSF-25 ($^{*\#\S\S}P<0.001$, $^{@}P<0.01$, $^{£}P<0.05$).

17.85±1.01) however, pancreatic sections from diabetic rats exhibited minimal/ no apparent insulin staining (% insulin staining area, 2.88±0.99; **Figure 4.8E**) which is consistent with active islet β cell destruction as revealed by H&E staining of these sections and is in agreement with the

decrease in cell viability and insulin secretion under the inflammatory conditions as observed in the *in-vitro* cell culture experiments (**Figure 4.6**). In rats treated with LSF-LA conjugate, insulin-positive cell clusters were significant and widely distributed throughout the pancreas despite evidence of persistent insulitis compared to normal control ($P<0.001$). Treatment with free LSF at 25 mg/kg (twice daily) showed increased insulin stained area compared to LSF dosed at 15 mg/kg (once daily) which is not significantly different from un-treated diabetic DC group.

4. Discussion

LSF is a potent anti-inflammatory and immunomodulatory agent but possesses challenging physico-chemical properties like high solubility and PK profile with a high rate of metabolism, poor bioavailability and rapid clearance, all necessitating a high dose and frequent dosing.[1,19,20] Due to these concerns associated with LSF, it is very challenging to encapsulate it in a delivery system and that might be a probable reason that no report is available on its formulation or delivery aspects in the literature. As the major shortcomings of LSF are attributed to its hydrophilic nature, we attempted to initially reduce the hydrophilicity of LSF by conjugating a hydrophobic moiety LA to it. This approach served another fundamental purpose which was to overcome the rapid metabolism of LSF to PTX since LA was attached to the free secondary hydroxyl group in side chain of LSF thus protecting this group which is mainly responsible for its rapid metabolism and clearance.[21] Further, a nano-sized self-assembling system of LSF-LA conjugate was attempted to harness the advantages of a nano formulation without use of any external excipient. LA is an essential fatty acid (18:2, ω-6) which cannot be synthesized by the human body and is hence supplemented from external sources to reap its benefits.[22,23] Apart from its health benefits, LA was selected as the fatty acid of choice since it has similar molecular weight (280.3 g/mol) as LSF. Taking advantage of its hydrophobic properties, it was conjugated to LSF in 1:1 ratio to form an

amphiphilic drug-fatty acid conjugate, which could self-assemble into micelles with hydrophobic core of LA with hydrophilic shell composed of LSF. This self-assembly provided various advantages of a nano delivery system including an altered uptake mechanism bypassing the first pass metabolism of LSF, prolonged residence time in the body, reduced clearance due to escape from the RES and ease of handling and storage and most importantly, no external surfactant/excipient was used for this purpose.

LSF-LA conjugate was synthesized by esterification using EDC.HCl-DMAP coupling reaction. In the synthesis process, ratio of different reactants was critically optimized after several trials to obtain the desired product, LSF-LA without any intermediates or impurities (unreacted EDC.HCl, DMAP, EDC-LA intermediate and free LSF). LA is a light sensitive molecule, so the reaction was carried out in dark conditions. It is critical to carry out the reaction between LA and EDC.HCl at 4 ℃ to precipitate out the byproduct which can otherwise interfere in reaction and could add a significant impurity to the final LSF-LA conjugate. Once intermediate is formed, it was confirmed by TLC followed by addition of LSF and reaction was further continued for 36 h at RT. A longer reaction time was necessary since the hydroxyl group of LSF is present in the alkyl side chain and is hence less reactive towards the carboxylic group of LA so the ester bond formation is slow; hence the reaction was continued for 36 h which resulted in a significant increase in the yield of final product as compared to yield obtained after shorter reaction times. Other reaction conditions were also optimized to maximize the reaction rate and yield of the product (65%). Further, LSF-LA conjugate was purified by flash column chromatography, wherein the ratio of solvents, hexane and ethyl acetate was optimized based on R_f value of reactants and final product as seen in TLC. We got >98 % purity of LSF-LA which was confirmed by HPLC. LSF-LA conjugate was characterized by various analytical techniques like TLC, ^{1}H NMR, ^{13}C

NMR, HR-MS, HPLC, FT-IR and DSC etc. all of which confirmed the formation of LSF-LA conjugate, its molecular weight, enhanced hydrophobicity and its purity (absence of free LSF and free LA in the final product).

LSF-LA conjugate self-assembled into nano-sized micelles (156.9 nm; PDI: 0.187) with a CMC of ≥ 1 μg/mL (1.84 μM) as confirmed by using pyrene as a fluorescent probe. The CMC value of LSF-LA conjugate was compared to a marketed micellar dispersion Hectorol® (a doxercalciferol intended for intravenous administration, comprising of poly(oxyethylene) sorbitan monooleate (Tween 80) as the micelle forming amphiphile. LSF-LA conjugate showed ten times lower CMC value (1.84 μM) than low molecular weight amphiphile, tween 80 (18 μM) indicating that micelles would remain stable *in vivo*.[24] Hydrolysis of LSF-LA conjugate was carried out in rat plasma to ensure that the ester bond present in the conjugate is able to undergo cleavage to release free LSF. Results showed that LSF-LA conjugate gets slowly hydrolyzed in rat plasma releasing 42.73% LSF within 72 h. Hydrolysis of the conjugate clearly indicates that the ester linkage of conjugate is easily cleavable such that the parent drug (LSF) is slowly released into the plasma which can possibly reduce the rate of interconversion between LSF and PTX in comparison to free LSF. It was also found that the same study when repeated by replacing plasma with other media like PBS (pH 7.4) containing 2% w/v ethanol or/and 5% w/v tween 80, showed negligible release of LSF from LSF-LA which proves the stability of the conjugate in other media. The aggregation number of the self-assembled micelles of LSF-LA was found to be 54 (at 30 times CMC) which further increased upon increasing the concentration of LSF-LA. The significance of aggregation number could be understood from the fact that self-assembled aggregates or micelles do not absorb directly but must dissociate into unimers for their absorption.[25] An optimum N_{agg} is desirable to ensure effective solubilization since a very high value of N_{agg} warns of a lesser

diffusion coefficient which could lower the rate of transport from air-water interfaces to the bulk of the medium thus hindering the solubilization of micelles.[12]

After systemic administration, nanomaterials are exposed to different physiological fluids including blood, wherein, several thousands of proteins present in the blood can bind or adsorb onto the nanoparticles (NPs) thus modifying their physicochemical properties such as size, surface charge, surface composition, and functionality. This gives a new biological identity to the NPs which represents its 'true identity' in the body and influences various biological responses such as fibrillation, cellular uptake, circulation time, bioavailability, and even toxicity.[26,27] The layer consisting of bound or adsorbed proteins around NPs is known as protein corona. In the present study, protein corona formation with LSF-LA SM was studied using BSA.[14] BSA is one of the most abundant proteins in humans and plays a dominant role in transport and disposition of a wide variety of different endogenous and exogenous compounds in blood.[28] Our primary goal was to assess the nature and extent of interaction of BSA (protein corona) with LSF-LA micelles in comparison to free LSF. LSF-LA SM and free LSF showed non-covalent binding with BSA possibly by static mechanism. Further, LSF-LA micelles showed lower binding constant (~3 times) when compared to free LSF with similar number of binding sites per BSA (*n*; 1.11 vs. 1.16) signifying a lower binding affinity and hence weaker interaction of LSF-LA micelles than LSF.[29] This indicates lesser recognition by RES and hence prolonged circulation time in the body along with availability of more amount of unbound LSF-LA to elicit its therapeutic response in the body which was further corroborated by the results of the PK and PD studies.

In-vitro efficacy of LSF-LA conjugate was tested on MIN-6 insulin secreting cells. Initially, LSF-LA conjugate was evaluated for cytotoxicity to check its safety after conjugating with fatty acid and it was found to be non-toxic to MIN-6 cells. LSF has been reported to protect

the pancreatic β -cells from cytokine-induced cell death by inhibiting the production of TNF-α, IL-1β, macrophage inflammatory protein (MIP)-1α, TGF-β and IFN-γ.[30,31] LSF-LA conjugate also protected the β–cells from cell death under inflammatory conditions and as compared to control and LSF alone showed ~40% and ~10% higher viability of cells. This enhanced viability of β–cells was also reflected in increased insulin secretion under inflammatory conditions in response to basal and stimulated levels of glucose. Further, after conjugation with LA and formation of micelles, the cellular uptake of LSF by MIN6 cells was significantly increased in comparison to free LSF. This could be attributed to the hydrophobicity of LA and self-assembly of LSF-LA into nano-sized micelles (156.9 nm) since cellular uptake is mainly influenced by size, shape, surface charge, and surface hydrophobicity.[32] Better uptake into the cells ensures more amount of LSF being available at the site of action for its therapeutic activity indicating possibility of dose reduction and hence lesser side effects.

T1DM develops when one or more immunoregulatory mechanisms fail, allowing auto-reactive T cells (one of the PBMCs) directed against islet β-cells to become active, to expand clonally, and to entrain a cascade of immune/inflammatory processes in the islet (insulitis), culminating in β-cell destruction.[33,34] Thus, in T1DM spontaneous proliferation of PBMCs, as well as a high production of cytokines such as IFN-γ, TNF-α etc. are observed. These inflammatory cytokines have been reported to show a direct β -cell cytotoxic effect in rodent islets.[35] In this study, PBMCs proliferation assay upon stimulation by mitogen stimulator PHA was carried out to assess effect of LSF and its fatty acid conjugate on proliferation of PBMCs wherein, in the presence of LSF and LSF-LA conjugate, a significant reduction in the proliferation of PBMCs was observed. LSF-LA conjugate also significantly decreased pro-inflammatory cytokines level (IFN-γ and TNF-α) in the conditioned media of PBMCs in comparison to free LSF treated cells.

Drug-lipid conjugation approach has demonstrated improvement in PK parameters of hydrophilic free drugs and hence improvement in their therapeutic action as observed in the case of gemcitabine conjugates developed by Jin and co-workers through the conjugation of lipid derivatives such as cholesterol-phosphonyl gemcitabine (CPNG) and N-octadecanonyl gemcitabine. The cytotoxicity of these nanoassemblies of gemcitabine was 3–6 folds higher than that of gemcitabine cytotoxicity as seen in five different human cancer cell lines due to amphiphilicity of CPNG.[36-38] Another example of drug-lipid conjugation is amphiphilic N-lauroyl-1-(3-chlorophenyl)-1,3-propanyl phosphonyl adefovir (LCPA) for the treatment of hepatitis where nanoassemblies showed the long-circulating and liver targeting effects according to the results of plasma PK and tissue distribution in the mice.[39] Similarly, a lipidated irinotecan conjugate was developed by Liang and co-workers that demonstrated increased cytotoxicity in cancer cells.[40] In our study, LSF was conjugated to LA, which exhibited a marked improvement in the PK parameters of free LSF such as $t_{1/2}$, MRT and Vz (~5 fold higher than free LSF). Furthermore, compared to free drug, LSF-LA conjugate showed a longer circulation time in the bloodstream due to escape from RES uptake. Similarly, in our *in vivo* efficacy studies, LSF-LA SM treated group exhibited a significant decrease in the level of fasting blood glucose and a notable increase in insulin level compared to free LSF treated group (even at a higher dose). Initially, 25 mg/kg, twice daily dose of LSF-LA conjugate was administered to the diabetic animals (based on literature reports for LSF) however, at this dose of LSF-LA, severe hypoglycemia was produced in the animals. So, the dose of LSF-LA conjugate was reduced to 15 mg/kg, once daily. Interestingly, compared to free LSF, treatment with LSF-LA conjugate stabilized the fasting blood glucose levels as well as corrected them to normal level in some animals. This might be attributed to the fact that LSF might have suppressed autoimmunity, giving the residual β-cells a chance to survive and thus

compensate for the lost of β-cells. LSF-LA conjugate also drastically reduced the levels of TNF-α and IFN-γ in the plasma; these proinflammatory cytokines are known to cause β-cell destruction by both CD4+ and CD8+ T lymphocytes.[41] Yoon et al[42] and Lee et al[43] have also reported that macrophages are mainly responsible for destruction of β-cells by producing proinflammatory cytokines such as TNF-α and IL-1β which further enhance T-cell proliferative responses and contributes to β-cell destruction.

The histological and immunohistochemical analysis were carried out to assess the difference in the anti-diabetic efficacy of free LSF in comparison to LSF-LA conjugate. Histological examination of H&E stained tissue sections indicated obvious differences in tissue morphology between control and treated groups. Upon STZ administration, necrosis and selective destruction of pancreatic islet β-cells were observed resulting in insulin deficiency. In untreated diabetic rats, degenerative and necrotic changes in pancreatic islets were seen, such as shrunken islets of Langerhans, hydropic degeneration, degranulation in the cytoplasm and lymphocyte infiltration. The nucleus of the necrotic cells indicated marginal hyperchromasia or pyknosis (**Figure 4.8C**). Our *in-vitro* results prove that LSF exhibited protective effect on pancreatic β-cells. Therefore, in the LSF-LA SM and free LSF (25 mg/kg, twice daily) treatment groups, however, most cells of the pancreatic islets were protected, although some degranulation, hydropic degeneration, necrosis was still observed, and the diameter of the islets of Langerhans was reduced. The rats treated with free LSF alone (15 mg/kg once daily), showed islet morphology similar to control diabetic group, indicating that free LSF at 15 mg/kg once daily is insufficient to protect the islets in pancreas. H&E staining and IHC analysis of pancreas confirmed β-cell protection and enhanced insulin secretion by LSF-LA conjugate as indicated earlier by cell culture studies in

MIN-6 cells. These results were also confirmed by quantification of insulin in plasma samples and calculation of % insulin stained area using ImageJ software.

5. Conclusion

LSF is a highly hydrophilic drug and shows poor PK parameters along with a high interconversion rate to PTX. In the present work, these problems have been resolved by conjugation of LSF to a hydrophobic moiety such as fatty acid through a biodegradable bond. Our results have demonstrated that as compared to free LSF, LSF-LA conjugate consisting of hydrophilic LSF and hydrophobic LA linked through an ester linkage exhibits a much better therapeutic effect in insulin secreting cells as well as in STZ induced T1DM model. Apart from the conjugation approach, the improvement in the therapeutic effect of the LSF-LA conjugate can also be attributed to its ability to self-assemble into micelles with an average hydrodynamic diameter of 156.9 nm in aqueous medium. The nanoscale characteristics of particles enabled escape from the RES as evident from the longer retention time and increased half-life of LSF-LA conjugate compared to that of free LSF in the bloodstream. Additionally, LSF-LA conjugate also reduced the LSF-PTX interconversion thus showing efficacy at a reduced dose and dosing frequency, which would eliminate the high-dose requirement for effective treatment of T1DM.

Bibliography

1. Striffler, J. S.; Nadler, J. L. Lisofylline, a novel anti-inflammatory agent, enhances glucose-stimulated insulin secretion in vivo and in vitro: studies in prediabetic and normal rats. *Metabolism* **2004,** *53*, (3), 290-296.
2. Yang, Z.; Chen, M.; Fialkow, L. B.; Ellett, J. D.; Wu, R.; Nadler, J. L. The novel anti-inflammatory compound, lisofylline, prevents diabetes in multiple low-dose streptozotocin-treated mice. *Pancreas* **2003,** *26*, (4), e99-e104.
3. Grasela, D. M.; Rocci, M. L. High-performance liquid chromatographic analysis of pentoxifylline and 1-(5'-hydroxyhexyl)-3, 7-dimethylxanthine in whole blood. *J Chromatogr.* **1987,** *419*, 368-374.
4. Wyska, E. Pharmacokinetic-pharmacodynamic modeling of methylxanthine derivatives in mice challenged with high-dose lipopolysaccharide. *Pharmacology* **2010,** *85*, (5), 264-271.
5. Lillibridge, J. A.; Kalhorn, T. F.; Slattery, J. T. Metabolism of lisofylline and pentoxifylline in human liver microsomes and cytosol. *Drug Metab. Dispos.* **1996,** *24*, (11), 1174-1179.
6. Wyska, E.; Pękala, E.; Szymura-Oleksiak, J. Interconversion and tissue distribution of pentoxifylline and lisofylline in mice. *Chirality* **2006,** *18*, (8), 644-651.
7. Cui, P.; Macdonald, T. L.; Chen, M.; Nadler, J. L. Synthesis and biological evaluation of lisofylline (LSF) analogs as a potential treatment for Type 1 diabetes. *Bioorg. Med. Chem. Lett.* **2006,** *16*, (13), 3401-3405.
8. Kingamkono, R. Role of animal sourced foods in human health and nutrition. *The role of biotechnology in animal agriculture to address poverty in Africa: Opportunities and challenges* **2006**, 247.
9. Raleigh, J.; Kremers, W.; Gaboury, B. Dose-rate and oxygen effects in models of lipid membranes: linoleic acid. *International Journal of Radiation Biology and Related Studies in Physics, Chemistry and Medicine* **1977,** *31*, (3), 203-213.
10. Jeevanandam, J.; San Chan, Y.; Danquah, M. K. Nano-formulations of drugs: recent developments, impact and challenges. *Biochimie* **2016,** *128*, 99-112.

11. Italiya, K. S.; Sharma, S.; Kothari, I.; Chitkara, D.; Mittal, A. Simultaneous estimation of lisofylline and pentoxifylline in rat plasma by high performance liquid chromatography-photodiode array detector and its application to pharmacokinetics in rat. *J. Chromatogr. B Analyt. Technol. Biomed. Life Sci.* **2017,** *1061*, 49-56.
12. Tehrani-Bagha, A. R.; Kärnbratt, J.; Löfroth, J.-E.; Holmberg, K. Cationic ester-containing gemini surfactants: Determination of aggregation numbers by time-resolved fluorescence quenching. *J Colloid Interface Sci.* **2012,** *376*, (1), 126-132.
13. Zhang, G.; Wang, A.; Jiang, T.; Guo, J. Interaction of the irisflorentin with bovine serum albumin: a fluorescence quenching study. *J. Mol. Struct* **2008,** *891*, (1-3), 93-97.
14. Guo, M.; Zou, J.-W.; Yi, P.-G.; Shang, Z.-C.; Hu, G.-X.; Yu, Q.-S. Binding interaction of gatifloxacin with bovine serum albumin. *Anal Sci* **2004,** *20*, (3), 465-470.
15. Gharagozlou, M.; Boghaei, D. M. Interaction of water-soluble amino acid Schiff base complexes with bovine serum albumin: fluorescence and circular dichroism studies. *Spectrochim. Acta A* **2008,** *71*, (4), 1617-1622.
16. Zhang, J.; Chen, L.; Zeng, B.; Kang, Q.; Dai, L. Study on the binding of chloroamphenicol with bovine serum albumin by fluorescence and UV–vis spectroscopy. *Spectrochim. Acta A* **2013,** *105*, 74-79.
17. Quah, B. J.; Warren, H. S.; Parish, C. R. Monitoring lymphocyte proliferation in vitro and in vivo with the intracellular fluorescent dye carboxyfluorescein diacetate succinimidyl ester. *Nature protocols* **2007,** *2*, (9), 2049-2056.
18. Rodríguez Galdón, B.; Pinto Corraliza, C.; Cestero Carrillo, J. J.; Macías Laso, P. Spectroscopic study of the interaction between lycopene and bovine serum albumin. *Luminescence* **2013,** *28*, (5), 765-770.
19. Wyska, E.; Świerczek, A.; Pociecha, K.; Przejczowska-Pomierny, K. Physiologically based modeling of lisofylline pharmacokinetics following intravenous administration in mice. *Eur. J. Drug Metab. Pharmacokinet.* **2016,** *41*, (4), 403-412.

20. Vieira, A.; Courtney, M.; Druelle, N.; Avolio, F.; Napolitano, T.; Hadzic, B.; Navarro Sanz, S.; Ben Othman, N.; Collombat, P. β-Cell replacement as a treatment for type 1 diabetes: an overview of possible cell sources and current axes of research. *Diabetes Obes. Metab.* **2016,** *18*, (S1), 137-143.
21. Yang, Z.; Chen, M.; Ellett, J. D.; Fialkow, L. B.; Carter, J. D.; Nadler, J. L. The novel anti-inflammatory agent lisofylline prevents autoimmune diabetic recurrence after islet transplantation1. *Transplantation* **2004,** *77*, (1), 55-60.
22. Anand, R.; Kaithwas, G. Anti-inflammatory potential of alpha-linolenic acid mediated through selective COX inhibition: computational and experimental data. *Inflammation* **2014,** *37*, (4), 1297-1306.
23. Johnson, M. M.; Swan, D. D.; Surette, M. E.; Stegner, J.; Chilton, T.; Fonteh, A. N.; Chilton, F. H. Dietary supplementation with γ-linolenic acid alters fatty acid content and eicosanoid production in healthy humans. *J. Nutr.* **1997,** *127*, (8), 1435-1444.
24. Uchegbu, I. F., *Low molecular weight micelles*. Springer: 2013; p 9-25.
25. Fletcher, P. D. Self-assembly of micelles and microemulsions. *Curr. Opin. Colloid Interface Sci* **1996,** *1*, (1), 101-106.
26. Lee, Y. K.; Choi, E.-J.; Webster, T. J.; Kim, S.-H.; Khang, D. Effect of the protein corona on nanoparticles for modulating cytotoxicity and immunotoxicity. *Int J Nanomedicine* **2015,** *10*, 97.
27. Van Hong Nguyen, B.-J. L. Protein corona: A new approach for nanomedicine design. *Int J Nanomedicine* **2017,** *12*, 3137.
28. Mote, U.; Bhattar, S.; Patil, S.; Kolekar, G. Interaction between felodipine and bovine serum albumin: fluorescence quenching study. *Luminescence* **2010,** *25*, (1), 1-8.
29. Yu, X.; Liu, R.; Ji, D.; Yang, F.; Li, X.; Xie, J.; Zhou, J.; Yi, P. Study on the synergism effect of lomefloxacin and ofloxacin for bovine serum albumin in solution by spectroscopic techniques. *J Solution Chem* **2011,** *40*, (3), 521-531.
30. Du, C.; Cooper, J. C.; Klaus, S. J.; Sriram, S. Amelioration of CR-EAE with lisofylline: effects on mRNA levels of IL-12 and IFN-γ in the CNS. *J. Neuroimmunol.* **2000,** *110*, (1), 13-19.

31. Van Furth, A.; Verhard, S., EM; Van Furth, R.; Langermans, J. Effect of lisofylline and pentoxifylline on the bacterial stimulated production of TNF-α, IL-1β and IL-10 by human leucocytes. *Immunology* **1997,** *91*, (2), 193-196.

32. Fröhlich, E. The role of surface charge in cellular uptake and cytotoxicity of medical nanoparticles. *Int J Nanomedicine* **2012,** *7*, 5577.

33. Herold, K. C.; Vignali, D. A.; Cooke, A.; Bluestone, J. A. Type 1 diabetes: translating mechanistic observations into effective clinical outcomes. *Nat. Rev. Immunol.* **2013,** *13*, (4), 243-256.

34. Kahanovitz, L.; Sluss, P. M.; Russell, S. J. Type 1 Diabetes-A Clinical Perspective. *Point of Care* **2017,** *16*, (1), 37-40.

35. Rabinovitch, A. Immunoregulatory and cytokine imbalances in the pathogenesis of IDDM: therapeutic intervention by immunostimulation? *Diabetes* **1994,** *43*, (5), 613-621.

36. Jin, Y.; Lian, Y.; Du, L.; Wang, S.; Su, C.; Gao, C. Self-assembled drug delivery systems. Part 6: in vitro/in vivo studies of anticancer N-octadecanoyl gemcitabine nanoassemblies. *Int. J. Pharm.* **2012,** *430*, (1), 276-281.

37. Li, M.; Qi, S.; Jin, Y.; Dong, J. Self-assembled drug delivery systems. Part 8: In vitro/in vivo studies of the nanoassemblies of cholesteryl-phosphonyl gemcitabine. *Int. J. Pharm.* **2015,** *478*, (1), 124-130.

38. Chitkara, D.; Mittal, A.; Behrman, S. W.; Kumar, N.; Mahato, R. I. Self-assembling, amphiphilic polymer–gemcitabine conjugate shows enhanced antitumor efficacy against human pancreatic adenocarcinoma. *Bioconjug. Chem.* **2013,** *24*, (7), 1161-1173.

39. Du, L.; Wu, L.; Jin, Y.; Jia, J.; Li, M.; Wang, Y. Self-assembled drug delivery systems. Part 7: Hepatocyte-targeted nanoassemblies of an adefovir lipid derivative with cytochrome P 450-triggered drug release. *Int. J. Pharm.* **2014,** *472*, (1), 1-9.

40. Zhang, C.; Jin, S.; Xue, X.; Zhang, T.; Jiang, Y.; Wang, P. C.; Liang, X.-J. Tunable self-assembly of Irinotecan-fatty acid prodrugs with increased cytotoxicity to cancer cells. *J. Mater. Chem. B* **2016,** *4*, (19), 3286-3291.

41. Amrani, A.; Verdaguer, J.; Thiessen, S.; Bou, S.; Santamaria, P. IL-1α, IL-1β, and IFN-γ mark β cells for Fas-dependent destruction by diabetogenic CD4+ T lymphocytes. *J. Clin. Invest.* **2000,** *105*, (4), 459-468.

42. Yoon, J.-W.; Jun, H.-S.; Santamaria, P. Cellular and molecular mechanisms for the initiation and progression of β cell destruction resulting from the collaboration between macrophages and T cells. *Autoimmunity* **1998,** *27*, (2), 109-122.

43. Lee, K. U.; Amano, K.; Yoon, J.-W. Evidence for initial involvement of macrophage in development of insulitis in NOD mice. *Diabetes* **1988,** *37*, (7), 989-991.